

Proceedings of the CTD/WIT 2019  
PROC-CTD19-088  
CMS CR-2019/041  
November 7, 2019

## The CMS Tracker Upgrade for the High-Luminosity LHC

ERNESTO MIGLIORE

*On behalf of the CMS Collaboration,  
Dipartimento di Fisica  
Università di Torino and INFN Sezione di Torino, Italy*

### ABSTRACT

The LHC machine is planning an upgrade program, which will smoothly bring the instantaneous luminosity to about  $5 - 7.5 \times 10^{34} \text{ cm}^{-2}\text{s}^{-1}$  in 2028, to possibly reach an integrated luminosity of 3000-4500  $\text{fb}^{-1}$  by the end of 2039. This High-Luminosity LHC scenario, HL-LHC, will require a preparation program of the LHC detectors known as Phase-2 upgrade. The current CMS Outer Tracker, already running beyond design specifications, and the recently installed CMS Phase-1 Pixel Detector will not be able to survive the HL-LHC radiation conditions. Thus, CMS will need completely new devices in order to fully exploit the high-demanding operating conditions and the delivered luminosity. The new Outer Tracker should also have trigger capabilities. To achieve such goals, the R&D activities have investigated different options for the Outer Tracker and for the pixel Inner Tracker. The developed solutions will allow including tracking information at the Level-1 trigger. The design choices for the Tracker upgrades are discussed along with some highlights on the technological choices and the R&D activities.

PRESENTED AT

Connecting the Dots and Workshop on Intelligent Trackers (CTD/WIT 2019)  
Instituto de Física Corpuscular (IFIC), Valencia, Spain  
April 2-5, 2019

# 1 Introduction

The goal of the High-Luminosity LHC program is to collect an integrated luminosity of  $3000 \text{ fb}^{-1}$ , optionally up to  $4500 \text{ fb}^{-1}$ , in about ten years of operations starting in 2028 and with a peak luminosity of  $7.5 \times 10^{34} \text{ cm}^{-2}\text{s}^{-1}$ . As the bunch crossing separation will stay the same as today (25 ns), the increase of instantaneous luminosity will result in up to 200 inelastic proton-proton collisions per bunch crossing (pileup) while the integrated luminosity will lead to an unprecedented hostile radiation environment. In the most exposed point in the Tracker volume, at  $r \simeq 3 \text{ cm}$  from the beamline, the expected fluence after  $3000 \text{ fb}^{-1}$  will reach  $2.3 \times 10^{16} \text{ 1 MeV n}_{\text{eq}}/\text{cm}^2$  and the corresponding total ionizing dose (TID) 12 MGy.

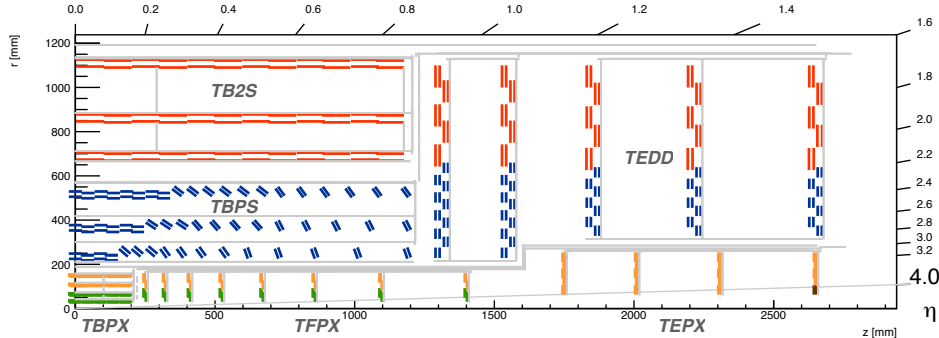


Figure 1: Sketch of one quarter of the layout of the CMS Tracker for HL-LHC in the  $r - z$  view. Inner Tracker 1x2 and 2x2 readout chips modules are shown in green and yellow respectively, Outer Tracker PS and 2S modules in blue and red. Details of the Inner Tracker and Outer Tracker modules can be found in the main text.

The proposed layout of the Tracker [1, 2] is shown in Fig.1: the Inner Tracker (IT) region,  $r < 20 \text{ cm}$  ( $r < 30 \text{ cm}$  for  $|z| > 120 \text{ cm}$ ), will be instrumented with high granularity pixel detectors guaranteeing an efficient pattern recognition in the high track density environment of HL-LHC; the Outer Tracker (OT) region will be instrumented with  $p_T$ -modules providing a  $\mathcal{O}(10)$  on-detector data reduction so that the precise measurements of the trajectories of charged particles from the Tracker can be used in the Level-1 (L1) trigger of the CMS experiment. Specifically, the main features of the upgraded Tracker will be:

- contribute to L1 trigger measuring at 40 MHz the momenta of charged particles and rejecting those with  $p_T < 2 \text{ GeV}/c$ ;
- be compatible with the upgraded L1 trigger of CMS which requires large readout bandwidth to withstand a 750 kHz L1 accept rate (currently about 100 kHz), and deep front-end buffers to comply with an increased L1 latency of  $12.5 \mu\text{s}$  (currently  $4 \mu\text{s}$ );
- ensure a robust two-track separation especially in high energy jets by means of a high granularity/low occupancy detector,  $\mathcal{O}(0.1\%)$  in the Inner Tracker and  $\mathcal{O}(1\%)$  in the Outer Tracker respectively;
- mitigate efficiently the pileup up to  $|\eta|=4$ ;
- guarantee an accurate measurement of the momentum and maintain a low level of fake tracks through optimal layout and reduced material budget.

The key ingredients to guarantee the functionality of the Tracker during the entire HL-LHC lifetime are:

- the deployment of dedicated sensors and ASICs;
- the operations of the sensors at the temperature of  $-20 \text{ }^\circ\text{C}$ ;
- a design which allows for full access to the Inner Tracker for maintenance and, optionally, for the replacement of the innermost layer of the barrel after half the HL-LHC timespan.

## 2 The Inner Tracker

The Inner Tracker is the main detector used in the offline track reconstruction for the pattern recognition. The IT will be made of hybrid pixel modules comprising a pixel sensor and two (1x2) or four (2x2) readout chips. The IT is structured into a barrel (TBPX) consisting of four layers with 9 modules/ladder and no projective gap at  $|\eta|=0$ , a forward (TFPX) made of 8(x2) small discs with 4 rings/disc, and a luminosity extension (TEPX) made of 4(x2) large discs with 5 rings/disc. The innermost ring of the last TEPX disc will be entirely devoted to the measurement of the bunch-by-bunch luminosity. Overall, the IT will cover a surface of about  $4.9 \text{ m}^2$  for a total of 2B channels.

### 2.1 Inner Tracker sensors and readout chip

**IT sensors.** High granularity will be achieved using small pitch pixel cells with either a rectangular ( $25 \times 100 \mu\text{m}^2$ ) or a square ( $50 \times 50 \mu\text{m}^2$ ) aspect ratio, both compatible with the same bond pattern (Fig. 2 (a)). The baseline choice for the sensor technology is to adopt planar n-on-p silicon sensors with 100-150  $\mu\text{m}$  active thickness. Results from TCAD simulations shown in Fig. 2 (b) indicate that charge above three times the foreseen threshold of the front-end chip can be collected up to a fluence of  $0.8 \times 10^{16} \text{ 1 MeV n}_{\text{eq}}/\text{cm}^2$ , that is approximately the fluence expected in the most exposed regions of the IT after half the HL-LHC timespan, operating the detector at 800 V. Since the sensors will be produced from single-side processing, no guard-rings on the backplane will limit the electric potential on the cut edge. Therefore protection mechanisms to avoid sparks between the readout chip, at ground potential, and the sensor are under investigation. For the innermost modules, usage of 3D silicon sensors, which allow efficient charge collection after irradiation operating at 150-200 V, is under consideration.

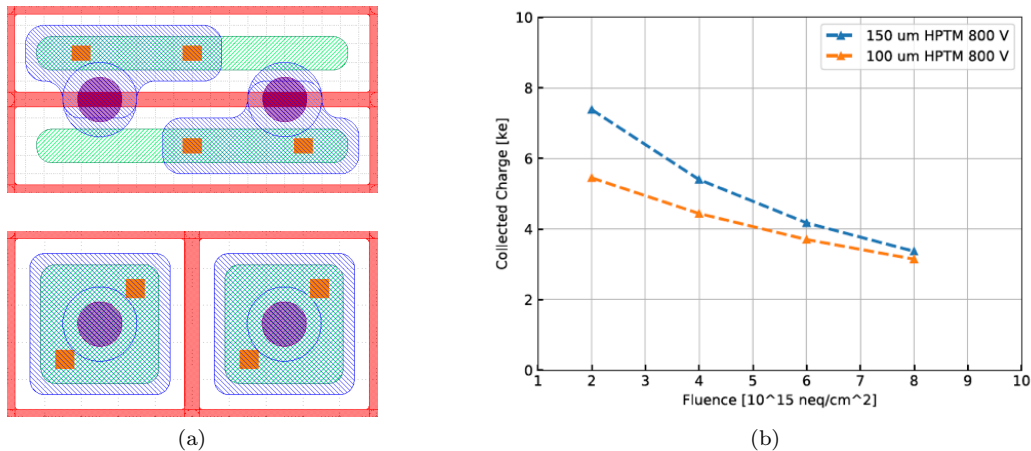


Figure 2: IT sensors: layout of the  $25 \times 100 \mu\text{m}^2$  and  $50 \times 50 \mu\text{m}^2$  pixel cells (a); simulated collected charge versus fluence in planar n-on-p pixel sensors biased at 800 V predicted by the *Hamburg Pentatrap Model* [3] (b).

**IT readout chip.** The readout chip (ROC) is required to operate with low noise at low thresholds ( $1000 e$ ) for efficient detection of signal on irradiated sensors, to sustain high hit rate (99% efficiency at  $3.2 \text{ GHz}/\text{cm}^2$ ) and to have high trigger rate capabilities (thanks to four  $1.28 \text{ Gb}/\text{s}$  output links). With the option of replacing the innermost layer of the TBPX, radiation tolerance requirements can be halved with respect to the  $12 \text{ MGy}$  TID expected for  $3000 \text{ fb}^{-1}$ . The ROC is currently being developed in CMOS 65 nm technology by the RD53/CERN collaboration [4, 5]. In 2018 a first prototype (RD53A) with dimensions  $1 \times 2 \text{ cm}^2$ , half-size of the final chip, has been delivered for standalone qualification and for use in single-chip assemblies with IT prototype sensors. All the three front-end architectures implemented in RD53A resulted fully functional after

a TID of 5 MGy. Measurements with X-rays show that the RD53A chip meets the required specifications on the hit rate [6]. Single chip assemblies with 3D sensors irradiated up to  $1 \times 10^{16}$   $1 \text{ MeV n}_{\text{eq}}/\text{cm}^2$  and exposed to 120 GeV/c proton beam at CERN SPS indicate that post-irradiation the decrease in the hit efficiency can be as low as 1% when operating the sensor at a moderate bias voltage of 150 V [7].

## 2.2 Inner Tracker modules

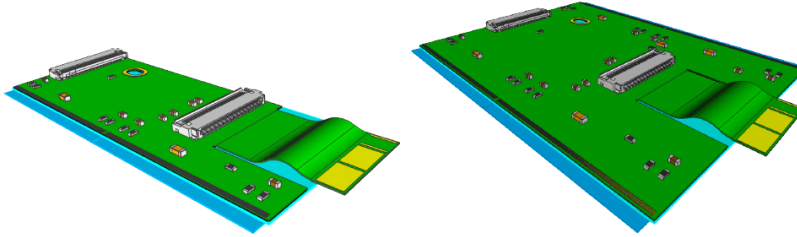


Figure 3: IT modules: rendering of the 1x2 (left) and 2x2 (right) readout chips modules.

Figure 3 shows the two types of modules, 1x2 and 2x2 ROCs, which will equip the IT. The module consists of the silicon sensor, a High-Density Interconnect circuit and the readout chip. To reduce the power loss in the cable with an acceptable cable mass, IT modules will be powered serially in groups of 8-12 modules each with the ROCs on the same module being powered in parallel. Since the ROC is the only ASIC present on the module, the 1.2 V required by the front-end is provided by a Low Drop Out (LDO) regulator integrated in the ROC together with a shunt designed to absorb the extra current flowing in case of a failure of one of the chips. Care in the design of the module is taken to guarantee that the cooling circuit is located under the region where the Shunt-LDOs, one for the analog and one for the digital domain, are placed in the ROC and hotspots in the power dissipation are expected.

## 3 The Outer Tracker

The Outer Tracker will measure in real-time all charged particles tracks with  $p_T > 2 \text{ GeV}/c$  for transmission to the L1 trigger. This will enable CMS to maintain low trigger rates, without lowering the efficiency for the physics of interest, even in the harsh environment expected at the HL-LHC. In the offline track reconstruction the OT will be the main detector for the measurement of the momentum of charged particles. The OT is arranged in a barrel made of two subsystems, TBPS for the innermost 3 layers and TB2S for the outermost 3 layers, and 5(x2) endcap discs (TEDD). The OT will cover a surface of about  $192 \text{ m}^2$  for a total of 42M strip and 170M macro-pixel channels.

### 3.1 Outer Tracker modules and sensors

**The  $p_T$ -modules.** The reduction required to limit the data volume sent out at the 40 MHz collision rate is achieved on the OT modules which are designed to reject signals from particles below a certain threshold on  $p_T$  exploiting the 3.8 T magnetic field of the CMS solenoid. A  $p_T$ -module is made of two silicon sensors with a small spacing in between: a flex hybrid routes data from both sensors to one ASIC which looks in a programmable search window for correlated clusters from the top and the bottom sensor. Only correlated clusters from high  $p_T$  tracks, “track stubs”, are read out at 40 MHz and sent to the L1 track finder (Fig. 4). Different sensor spacings, from 1.6 mm up to 4 mm, guarantee a homogeneous selection of the  $p_T$ -threshold in different regions of the OT. Furthermore, TBPS adopts a tilted barrel geometry to guarantee full efficiency for stubs from inclined tracks which otherwise would cross top and bottom sensors in different modules.

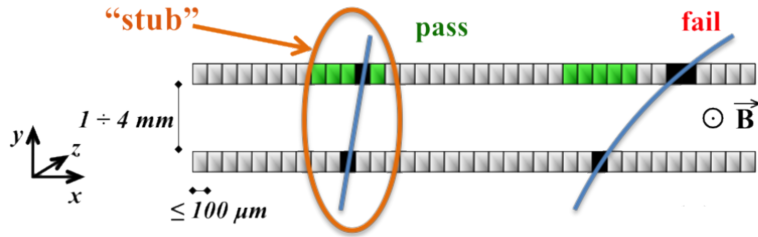


Figure 4: Sketch of a  $p_T$ -module showing the concept of stub selection.

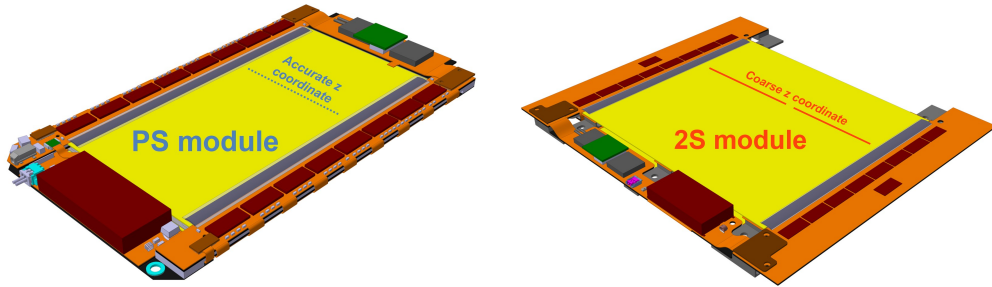


Figure 5: OT modules: rendering of the PS (left) and 2S (right) modules.

Two module types are foreseen for the OT (Fig. 5):

- PS modules equipping the TBPS and the innermost TEDD rings. A PS module is composed of one strip sensor (two rows of 960 AC-coupled strips with dimensions  $2.35 \text{ cm} \times 100 \mu\text{m}$ ) and a one macro-pixel sensor (30 720 DC-coupled pixels with dimensions  $1.5 \text{ mm} \times 100 \mu\text{m}$ ).
- 2S modules equipping the TB2S and the outermost TEDD rings. A 2S module is composed of two strip sensors (two rows of 1016 AC-coupled strips with dimensions  $5 \text{ cm} \times 90 \mu\text{m}$  per sensor).

As no aggregator cards are foreseen between the module and the back-end, OT modules are self-contained units made of the two sensors, the Front-End Hybrids with the readout and concentrator ASICs, the Service Hybrids hosting the DC-DC power converters and the data-links, and the spacers providing the proper lever-arm between the two sensors. To guarantee the correct functioning of the stub finding procedure, the maximum rotation allowed between the top and the bottom sensor is  $400 \mu\text{rad}$  in 2S modules and  $800 \mu\text{rad}$  in the shorter PS modules.

**The OT sensors.** Since all the front-end ASICs of the OT adopt a binary readout architecture, the relevant figure-of-merit for the OT sensors is the charge collected after irradiation on a single “seed” channel. This poses more stringent constraints on the strip sensors used for 2S module and for the PS-strip module which are readout with ASICs with larger equivalent noise charge (ENC) values (ENC=1000 e in case of the CBC chip used for the 2S sensors and ENC=700 e for the SSA chip used for the PS-strip sensors). Figure 6 shows the signal on the seed strip as a function of the bias voltage for n-in-p strip sensor prototypes irradiated at fluence between 1.5 and 2 times the fluence expected in TBPS and TB2S after  $3000 \text{ fb}^{-1}$ : assuming a threshold 4 times the ENC, sensors with  $200\text{--}240 \mu\text{m}$  active thickness operated at the nominal bias voltage (600 V) guarantee to collect a charge 3 times larger than the threshold at the end of the HL-LHC operations. For the sensors used for the macro-pixels, the front-end ASIC (MPA) has a much lower noise figure (ENC=200 e). In this case  $200 \mu\text{m}$  thick sensors are sufficient to guarantee the requested charge.

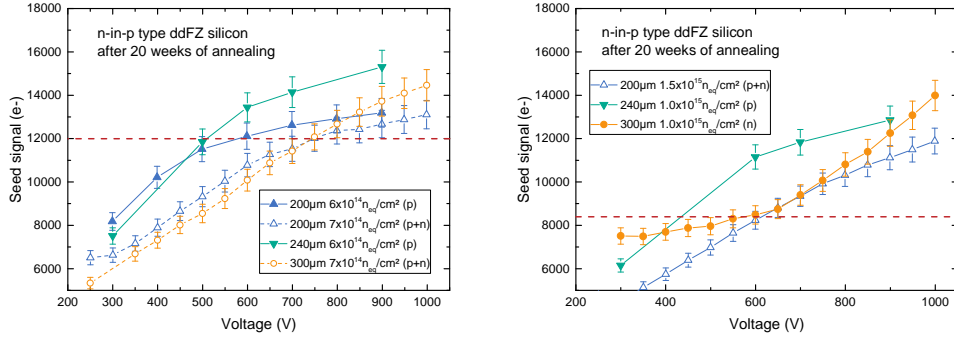


Figure 6: OT sensors: charge collected on the seed strip as a function of the bias voltage at fluences relevant for the 2S (left) and PS (right) modules respectively. Sensors were irradiated up to the nominal fluence with 23 MeV protons (“p”) or with protons plus reactor neutrons (“p+n”). The horizontal dashed line represents the envisaged seed signal charge (12000 e for 2S modules and 8400 e for PS modules respectively).

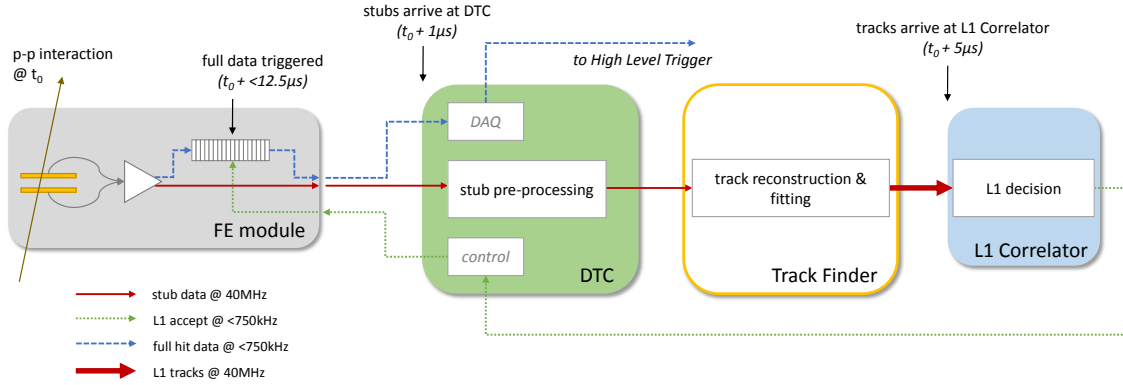


Figure 7: Sketch of the data flow from OT modules to the CMS L1 trigger.

### 3.2 Outer Tracker back-end electronics

A schematic overview of data flow from the Tracker to the CMS L1 trigger is shown in Fig. 7. Stubs from up to 72 OT modules are sent through optical fibers to one Data Trigger and Control board (DTC) which unpacks the stubs and converts the information from local to global coordinates. The DTC forwards the data, sliced in space and in time, to a Track Finder Processor (TFP). Each input of the TFP collects the data stream from a single event and from two overlapping nonants in which the OT is cabled. Pattern recognition and track finding is performed by the TFP using commercially available FPGAs. Two different approaches for the pattern recognition and track fitting have been perfected after the TDR and verified in real life on two TFP hardware demonstrators. Both the systems have proved to be fully functional delivering tracks to the L1 trigger system within the allotted time-budget of  $4 \mu\text{s}$ . Currently, a hybrid approach combining the best of both algorithms is under study [8].

## 4 Common aspects and performance

The amount of material in the Tracker volume impacts the accuracy on the measurement of the track transverse momentum and the rate of fake tracks and ultimately it is related to the power required to operate the detector, as high power consumption requires more massive cables for the power distribution and a more complex cooling system for efficient heat dissipation. Despite the estimated power consumption

for the upgraded Tracker is three times larger than for the current Tracker, 50 kW for the IT and 100 kW for the OT, careful choices for the powering scheme (serial powering for the IT and use of DC-DC converters for the OT) and for the cooling system (use of two-phase evaporative CO<sub>2</sub> cooling which allows to use steel cooling pipes with a reduced diameter of about 2 mm) result in a profile of the material which is even better than for the current detector. The beneficial effect on the resolution on the track transverse momentum and on the impact parameter in the transverse plane is shown in Fig. 8: the upgraded Tracker is expected to achieve better performance than the current detector on an extended pseudo-rapidity range despite the higher pileup expected at the HL-LHC.

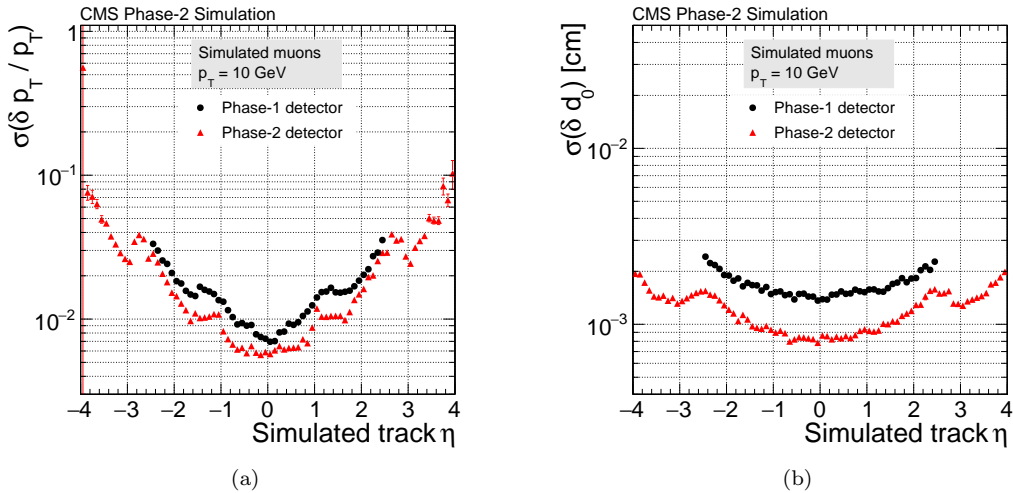


Figure 8: Comparison of expected resolution on track parameters between the current (Phase-1) Tracker and the HL-LHC (Phase-2) Tracker using single isolated muons with  $p_T=10$  GeV/c: transverse momentum (a) and impact parameter in the transverse plane (b).

## 5 Conclusions

For the HL-LHC the entire Tracker of the CMS experiment will be replaced with a new detector which besides having an unprecedented radiation tolerance will guarantee an efficient online selection and offline reconstruction of events up to an average pileup of 200 events per bunch crossing. For the OT the main design choices have been already established. For the IT crucial decisions like the choice of the architecture of the front-end chip or the technology of the sensors will be taken in the next months, mid-2019 and end of 2020 respectively, based on the results from prototypes that for the first time were operated after being exposed to radiation levels comparable with those expected at HL-LHC. In the next years the project will move to the large-scale production of the components (4k IT modules and 14k OT modules). Quality assurance during production and care to system aspects in the integration of the different subsystems will be crucial to guarantee the expected performance of the upgraded Tracker.

## References

- [1] The CMS Collaboration, “Technical Proposal for the Phase-II Upgrade of the CS Detector”, CERN-LHCC-2015-010, LHCC-P-008 (2015).
- [2] The CMS Collaboration, “The Phase-2 Upgrade of the CMS Tracker - Technical Design Report”, CERN-LHCC-2017-009, CMS-TDR-014 (2017).

- [3] J. Schwandt et al., “A new model for the TCAD simulation of the silicon damage by high fluence proton irradiation - The Hamburg Penta Trap Model”, proceedings of IEEE-NSS-MIC-2018 2018 IEEE Nuclear Science Symposium and Medical Imaging Conference (2019).
- [4] J. Chistiansen, M. Garcia-Sciveres, “RD Collaboration proposal: Development of pixel readout integrated circuits for extreme rate and radiation”, CERN-LHCC-2013-008; LHCC-P-006 (2013).
- [5] RD53 Collaboration, “RD53A Integrated Circuit Specifications”, CERN-RD53-PUB-15-001 (2015).
- [6] D. Ruini on behalf of the CMS Tracker group, “Serial Powering for the Phase 2 upgrade of the CMS pixel detector”, CMS CR-2019/009 (2019).
- [7] J. Duarte Campderros on behalf of the CMS Tracker group, “Results on Proton-Irradiated 3D Pixel Sensors Interconnected to RD53A Readout ASIC”, CMS CR-2019/028 (2019).
- [8] T. James on behalf of CMS L1 Track Finding group, “Level-1 track finding with an all-FPGA system at CMS for the HL-LHC”, these proceedings.